Thermochimica Acta 488 (2009) 1–9

Contents lists available at ScienceDirect

Thermochimica Acta

journal homepage: www.elsevier.com/locate/tca

Heat release measurements on micron and nano-scale aluminum powders

Alexander B. Morgan*, J. Douglas Wolf, Elena A. Guliants, K.A. Shiral Fernando, William K. Lewis*

University of Dayton Research Institute, 300 College Park, Dayton, OH 45469, United States

ARTICLE INFO

Article history:
Received 9 December 2008
Received in revised form 7 January 2009
Accepted 12 January 2009
Available online 22 January 2009

Keywords:
Oxygen consumption calorimetry
Nanoparticles
Pyrolysis

ABSTRACT

Aluminum nanoparticles are a focus of active research largely due to their attractive oxidation energetics and fast reaction kinetics compared with micron-scale or larger particles. A large number of different aluminum powders are currently available and the present study reports the results from a side-by-side comparison of several representative types of aluminum nanoparticles. Conventional oxide-passivated micron-scale and nano-scale powders, as well as organically passivated nanoparticles were studied using pyrolysis combustion flow calorimetry (PCFC) at temperatures up to 700 °C. The reaction onset temperature and extent of oxidation were observed to depend on particle size. A multi-step oxidation process was observed, with the individual steps becoming increasingly pronounced at smaller particle sizes. The results from PCFC testing gave useful insight into the oxidation behavior of these materials, especially the organic passivated particles, but, under these oxidation conditions the materials were not fully oxidized.

1. Introduction

Nanoscale aluminum particles have become a recent focus of active research due to their high heat of reaction and fast reaction kinetics compared to micron-scale or larger particles [1–6]. Because such particles are highly reactive, they are typically passivated by a naturally occurring aluminum oxide shell. While the oxide shell represents only a small fraction of the particle mass for micron and larger particles, for nanoparticles the contribution of oxide to particle mass can become quite large. Ultimately, this limits the energy that can be obtained by oxidation of the nanoparticle. To solve this problem, alternative methods such as passivation using an organic layer are currently being explored [7–14]. To date, a number of different types of aluminum powders are available either commercially or from active research groups. The purpose of the current study is to perform a side-by-side comparison of the oxidation of several representative types of aluminum particles, including normal oxide-passivated commercial samples, as well as those passivated by an organic shell.

Oxidation processes involving aluminum particles have been the subject of several detailed investigations [2,5,15]. These studies have utilized methods such as differential scanning calorimetry (DSC), and thermogravimetric analysis (TGA), which are widely used and well-understood techniques. However, for the organically passivated samples mentioned above, these techniques suffer from the drawback that it can be difficult to distinguish between organic heat release and metal heat release, especially if they occur simultaneously. In the present investigation we wish to study the oxidation of conventional aluminum particles as well as those protected by organic coatings. As a result, it is highly desirable to utilize a technique that can separate the contributions to the overall oxidation process arising from reaction of the metallic and organic components of the latter. To achieve this separation, we have used pyrolysis combustion flow calorimetry (PCFC) to study the oxidation of the nanoparticle samples.

Pyrolysis combustion flow calorimetry is a technique that measures heat release by monitoring oxygen consumption as the sample reacts/combusts. The heat release associated with the observed oxygen depletion is then calculated from a relation appropriate to the material undergoing oxidation, as we will discuss in detail below. One advantage to this technique is the small sample size required (5–50 mg) which is ideal for research efforts when initial work only yields small amounts of nanoparticles. Additionally, when the sample is reacted in an air atmosphere, this technique can isolate oxide-forming reactions from nitride-forming reactions. But the key advantage of this method is that the combustion of volatile and non-volatile components of a sample can be measured separately. Briefly, the technique works as follows. A sample is exposed to fast heating under an inert gas flow (100% N_2), pyrolyzing any organic products, and the volatile decomposition products are then pushed into a high temperature combustion furnace where they are mixed with a synthetic air blend (80% N_2 and 20% O_2). An oxygen sensor downstream records the oxygen depletion resulting from combustion reactions. In this mode of operation, only species that are volatile at the pyrolysis temperature may contribute to the O_2 depletion signal. Alternatively, the sample is heated in the presence of synthetic air (80% N_2 and 20% O_2), and the gas flow is then

* Corresponding author.
E-mail addresses: alexander.morgan@udri.udayton.edu (A.B. Morgan), william.lewis@udri.udayton.edu (W.K. Lewis).

0040-6031/$ – see front matter © 2009 Elsevier B.V. All rights reserved.
doi:10.1016/j.tca.2009.01.016

routed through the furnace to the oxygen sensor as before. In this mode, both volatile and non-volatile portions of the sample contribute to the oxygen depletion. PCFC is a standardized technique, ASTM D7309-07, and is sometimes referred to as micro-combustion calorimetry (MCC). Additional references on the PCFC and some of the other work that has been undertaken with this instrument are included at the end of this article in the reference section [16–22]. In this study, the PCFC technique was used to measure the heat release of five aluminum powder samples (three nanoscale, one micron sized, and one nanoscale coated with oleic acid) and an oleic acid control sample using both modes of operation.

2. Experimental procedures

The five aluminum powder samples used in this study are described as follows:

- Micron-Al: 100 μm size powder, grey color. Purchased from Strem Inc.
- Nano Al-100A nanoparticles: 100 nm size powder, dark grey color. Purchased from Aldrich.
- Nano Al-100B nanoparticles: 100 nm size powder, dark grey color. Purchased from Alfa Aesar.
- Nano Al-10 nanoparticles: 10–20 nm size powder, dark grey color. Purchased from MTI.
- Nano Al-OA nanoparticles: aluminum metal nanoparticles coated with oleic acid shell. Synthesized via sonochemistry at UDRI/WPAFB [10].

All samples were weighed using a Mettler-Toledo UM-3 microbalance and small metal spatula. The oleic acid sample had to be metered out using a micropipetter since it was a liquid at room temperature. These materials were subjected to TEM, XRD for nanoparticle analysis and PCFC for heat release/oxygen consumption measurements.

Transmission electron microscopy studies (TEM) images were obtained using a Hitachi H-7600 instrument. First the nanoparticle powder samples were sonicated in hexane to disperse and then these solutions were spotted onto a 300 mesh carbon coated grid. All the TEM images were taken at 100 kV accelerated voltage.

X-ray powder diffraction (XRD) analysis was performed on a Bruker D8-Advanced equipped with a Cuα source and Sol-X detector. For analysis solid powder samples were placed on a zero-background holder. In typical analysis, the scans were run over a 2θ range from 5° to 85°, with an angle increment of 0.05° and the collection time of 5 s/angle increment.

All aluminum powder samples were tested with PCFC on a MCC-1 unit (Govmark Organization Inc., Farmingdale, NY), shown schematically in Fig. 1. Samples were tested as per ASTM D7309-07. A 3–4 mg sample was placed in the Specimen Chamber and heated at 1 °C/s to 700 °C. Two methods from ASTM D7309-07 were used to study the samples. In method A, the pyrolyzer gas flow was set to 100% N_2. Volatile decomposition species produced during heating are pushed into a 900 °C combustor, where the atmosphere is set to a 20% O_2/80% N_2 mixture, which is a composition very close to that of air. Oxygen depletion resulting from combustion reactions are monitored using an oxygen sensor downstream. Since the volatility of aluminum is low below 700 °C [25], we would not expect it to reach the combustor, hence use of method A should give no measured heat release for aluminum metal, but will be able to measure the heat release from combustion of the oleic acid coating on the Nano Al-OA sample, as well as any heat release generated by pyrolysis of our oleic acid control sample. In method B, both pyrolyzer and combustor gas composition set to a 20% O_2/80% N_2 mixture. Oxygen depletion is measured as in method A. In this configuration,

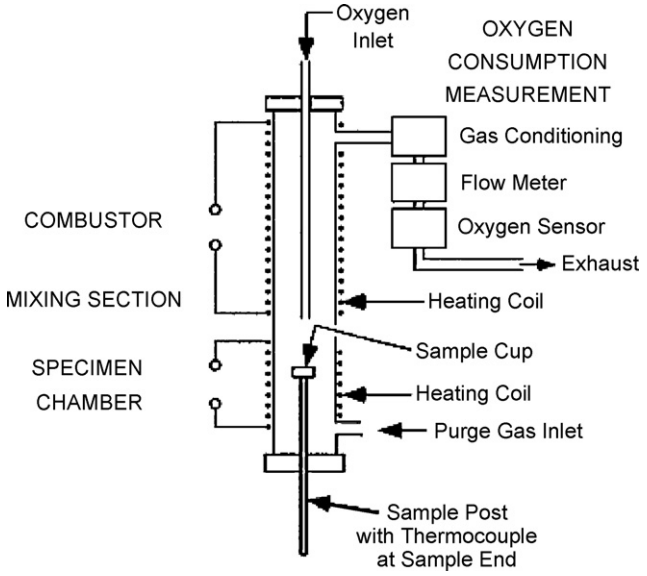

Fig. 1. Schematic representation of pyrolysis combustion flow calorimetry (PCFC) instrument.

the entire sample is exposed to oxidizing conditions and the resulting signal should contain contributions from reaction of aluminum metal as well as any organic material.

As mentioned above, in the PCFC technique heat release is calculated from the observed oxygen consumption. Thornton [23] has shown that for most organics, the net heat of combustion per gram of oxygen consumed is remarkably constant at 13.1 ± 0.6 kJ/g O_2. This relation, known as Thornton's rule [24], is used to calculate heat release from the observed oxygen consumption for organic samples. For the oxidation of aluminum, we instead use the heat of reaction associated with formation of Al_2O_3, namely 34.9 kJ/g O_2 consumed [25], to calculate the heat release from aluminum containing samples.

All commercial aluminum powders studied in this project were used as received. The oleic acid control sample was tested under identical conditions to the aluminum powder samples and was also used as received. All samples were tested in triplicate, with the exception of the oleic acid sample, which was tested in quadruplicate due to some observed scatter during testing.

3. Results and discussion

3.1. Nanoparticle characterization

Before collecting heat release data on the aluminum nanopowders, they were characterized in terms of their particle size, chemical composition, crystal structure, and morphology. X-ray diffraction analysis was used to identify the composition of the samples and the particles' crystallinity while transmission electron microscopy (TEM) was instrumental in evaluating the size of the particles, their size distribution, and the overall sample's morphology.

Fig. 2 shows representative TEM images taken for two different Nano Al-100 samples. Although the average particle size appears to be similar for both samples, Nano Al-100A demonstrates a broader size distribution. Both samples contain approximately spherical particles with diameters in the range of ~60–150 nm for Nano Al-100B and ~30–250 nm for Nano Al-100A, respectively. However, compared to the obviously large Micron-Al sample in Fig. 3(left), these samples can clearly be considered nanoscale in size. The Nano Al-10 sample (Fig. 3, right) does indeed have some small

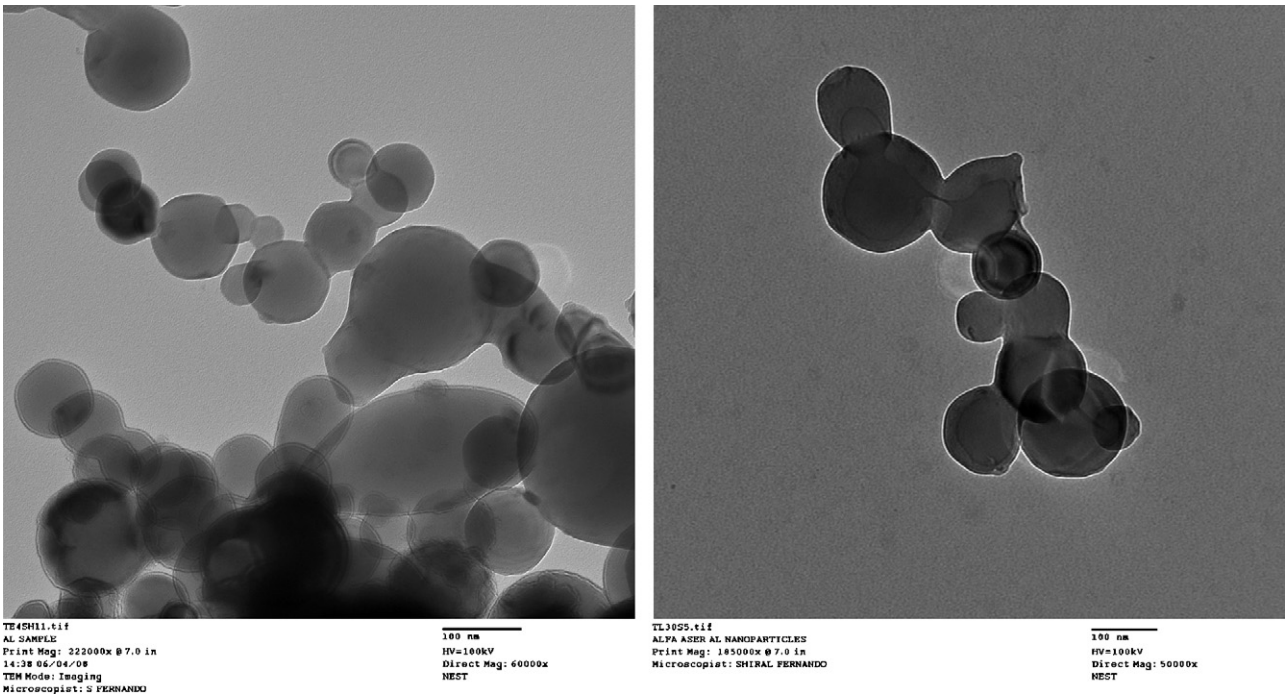

Fig. 2. TEM images of Nano Al-100A (60,000× mag., left) and Nano Al-100B (50,000× mag., right).

10 nm sized nanoparticles present, but it also has larger particles and a predominance of rod-shaped nanostructures in comparison to the spherical shapes of the other aluminum nanopowder samples. The aluminum-oleic acid core-shell nanoparticles (Fig. 4) are the smallest, showing an average size of ∼30 nm and the size distribution of ∼10–70 nm (Fig. 4) but agglomerates of larger sizes can be seen in the micrograph. Only the Micron-Al sample appears to be relatively aggregate free; the smaller particles in the rest of the samples readily aggregate during or after synthesis.

The results of XRD analysis of one of the commercial samples and our Al oleic acid core-shell nanoparticles is represented by the spectra obtained for Nano Al-100B and Nano Al-OA in Fig. 5. Each spectrum is characterized by five narrow features in the vicinity of 38°, 45°, 65°, 78° and 82°, respectively. The peaks in this spectrum are well matched with face-centered-cubic aluminum (0) [26]. The evident high intensity and narrowness of the peaks in both spectra imply a high degree of crystallinity. The broad peak centered at 22° of Nano Al-OA sample most likely originates from oleic acid [10]. In addition to these peaks, minor peaks appeared in some

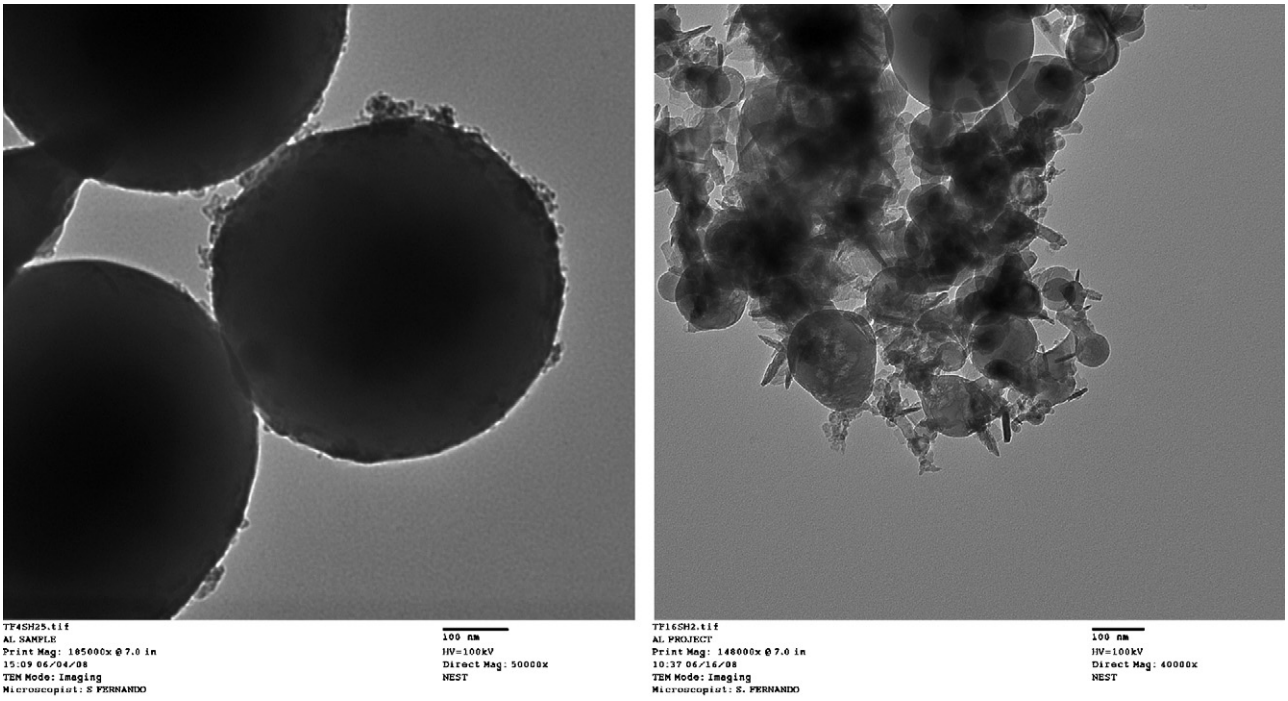

Fig. 3. TEM images of Micron-Al (50,000× mag., left) and Nano Al-10 (40,000× mag., right).

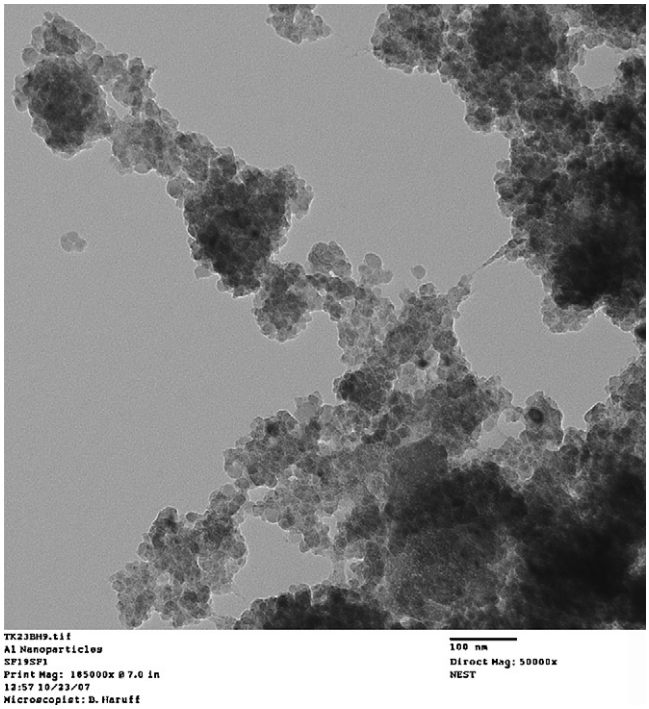

Fig. 4. TEM image of Nano Al-OA (50,000× mag.).

of the commercial aluminum samples which do not match with the pattern for any well-characterized phase of aluminum oxide. The lack of well defined oxide signals suggests that any oxide on these aluminum particles is either of too low a concentration to be detected, or, is amorphous in nature and does not yield a coherent XRD signal [2]. These XRD data suggest that the aluminum samples used in this study contain significant amounts of zero-valent FCC aluminum.

3.2. Nanoparticle oxygen consumption calorimetry studies

Results from the PCFC experiments on each of the materials are collected in Table 1. The data in the table covers the following measurements:

- Char yield: This is obtained by measuring the sample mass before and after pyrolysis.
- Char notes: Description of the sample residues collected from each test.
- Total heat release (HR) for combustion of organic: Calculated from the observed oxygen depletion using Thornton's rule (13.1 kJ/g O_2) [23,24]. The precision of the oxygen consumption measurements is expected to be in line with those listed in the ASTM D 7309-07 standard for the PCFC technique, and is estimated to be ±6%.
- % Sample consumed (via organic combustion): Estimate of the percentage of the sample reacted obtained from the ratio of the measured total HR (kJ/g) to the theoretical HR expected assuming all of the sample undergoes complete combustion.
- Total HR for oxidation of Al metal: Calculated from observed oxygen depletion using heat of reaction of Al metal to form Al_2O_3 (34.9 kJ/g O_2) [25]. We estimate that the heat release values listed in the table are accurate to approximately 10%.
- % Sample consumed by Al oxidation: Estimate of the percentage of sample reacted obtained from the ratio of the measured total HR (kJ/g) to the theoretical HR expected assuming the entire sample mass undergoes complete oxidation to form Al_2O_3. Theoretical heat release for this reaction is 31 kJ/g Al burned [25].
- % Sample consumed calculated by mass change: Estimate of the percentage of the sample reacted obtained from the measured char yield, assuming that the observed mass increase is the result stoichiometric oxidation of Al to form Al_2O_3.

Before discussing the aluminum nanoparticle data, it should be mentioned that this technique was originally developed to measure combustion of organic samples [20] and with that in mind, we

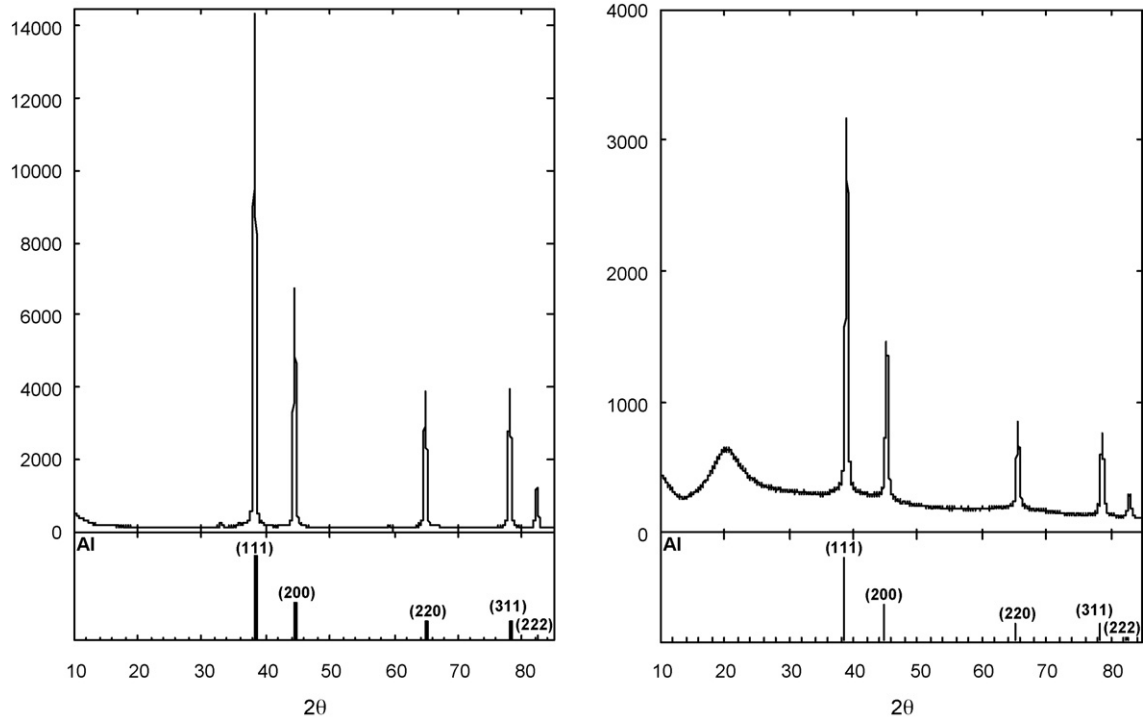

Fig. 5. XRD data of Nano Al-100B (left) and Nano Al-OA (right).

Table 1
Char yield, calculated heat release, and extent of reaction (average of 3–4 runs) for aluminum nanoparticles.

Sample (atmosphere)	Char yield (wt.%)	Char notes	Total HR (organic) (kJ/g)	% Sample consumed (organic combustion)	Total HR (Al oxidation) (kJ/g)	% Sample consumed	
						Al oxidation	From mass change
Neat oleic acid (nitrogen)	0.2	Little brown film around bottom	32	87	–	–	–
Neat oleic acid (air)	3.6	Black film all over pan	32	87	–	–	–
Micron-Al (nitrogen)	100	Grey powder to silvery beads	–	–	0	0	–
Micron-Al (air)	111	Brownish ash, no white	–	–	1	3	13
Nano Al-100A (nitrogen)	103	Grey powder to black powder	–	–	0	0	–
Nano Al-100A (air)	135	Light grey powder, some white ash	–	–	7.4	24	39
Nano Al-100B (nitrogen)	108	Grey powder to black powder	–	–	0	0	–
Nano Al-100B (air)	137	Light grey powder, some white ash	–	–	9.8	32	42
Nano Al-10 (nitrogen)	115	Grey powder to black powder	–	–	0	0	–
Nano Al-10 (air)	123	Light grey powder, some white ash	–	–	6.2	20	26
Nano Al-OA (nitrogen)	61	Black powder unchanged	8.3	23	–	–	–
Nano Al-OA (air) peak #1	69	Dark grey, some white ash	9.2	25	24.5	79	–
Nano Al-OA (air) peak #2	69	Dark grey, some white ash	–	–	1.9	6	–

tested oleic acid by itself under air and nitrogen pyrolysis conditions to verify proper operation of the instrument. Further, the combustion behavior of the oleic acid is directly related to the organically coated aluminum nanopowders discussed below since oleic acid was used to coat the nanoparticle's aluminum core. From Table 1, the total heat release of oleic acid is measured by PCFC to be 32 kJ/g, and this value is reasonably close to the reported heat of combustion for oleic acid of 39.4 kJ/g [27,28]. It is noteworthy that this value is independent of initial atmosphere (nitrogen or air) and that the shape of the heat release curves, seen in Fig. 6, are very similar in both cases with the peak heat release value occurring at practically the same temperatures. Interestingly, there is more residue left behind under air conditions (3.6% char yield in air versus 0.2% in nitrogen) which suggests some incomplete combustion under these conditions. Still, even with the small amount of incomplete combustion we can state that the instrument is working properly, pyrolyzing most of the sample and yielding reasonable heat release values.

When studying the micron-sized aluminum powder, we see from Table 1 that under nitrogen conditions there is no heat release observed (no oxygen consumed). This makes sense because Al is non-volatile at the temperatures studied and cannot be carried to the 900 °C combustion furnace. Under the 80% N_2/20% O_2 (air) conditions, we observe oxidation in Fig. 7(left) around 620 °C, similar to results reported by Trunov et al. [2]. From the oxygen consumption, we determine that we only measured 1.0 kJ/g of total heat release for the Micron-Al sample, compared with the theoretical value of 31 kJ/g Al [25], which implies incomplete oxidation of the sample. Using the measured heat release, we can estimate that only 3% of the metal was oxidized. Incomplete combustion is supported by the measured weight increase in the char yield, as there was only an 11 wt.% increase. Complete stoichiometric reaction would increase the sample mass by 89 wt.%, so using the weight gain numbers we can estimate a 13% oxidation of the Micron-Al sample. Although these estimates are a bit different, they agree that the vast majority of the sample remains unreacted. Further confirmation that the sample was not fully oxidized is found in the fact that the Micron-Al sample at the end of the test was brown in color, whereas Al_2O_3 is white in color. Of course, this result is not surprising since it has been shown previously that oxidation is incomplete at these temperatures [2].

For the Nano Al-100A and Al-100B samples, we again observe (Table 1) no heat release under nitrogen pyrolysis conditions but do observe some weight gain in the recovered sample, likely due to the formation of AlN [29,30]. Since there is more surface area available with this material compared to the Micron-Al

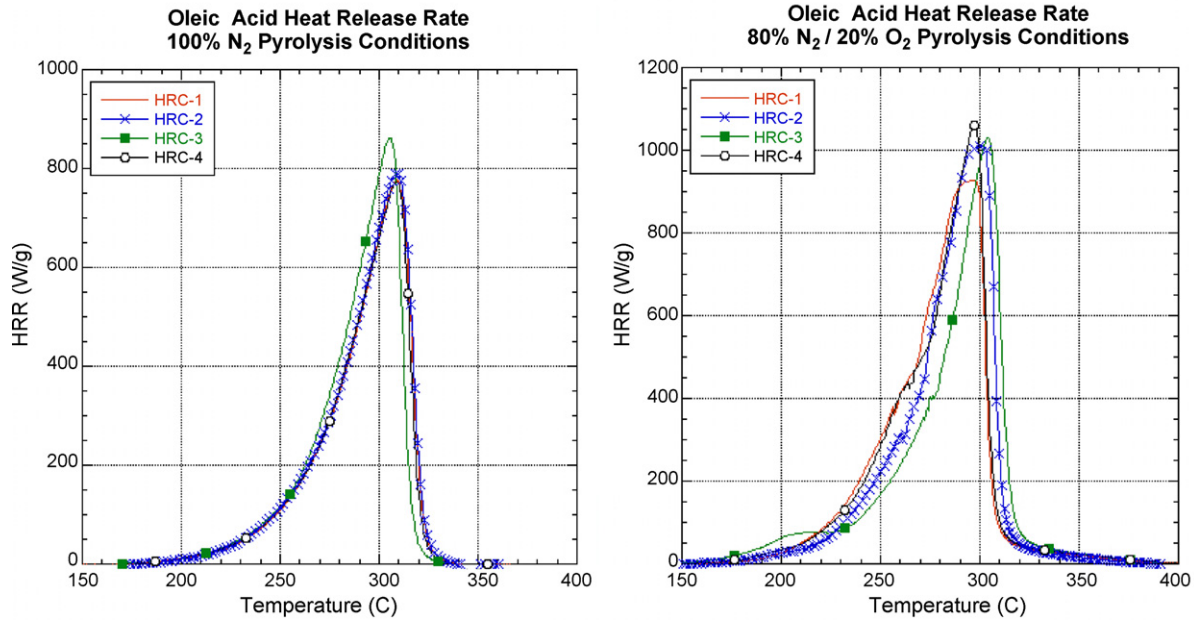

Fig. 6. Heat release rate curves, oleic acid pyrolyzed under N_2 (left) or 80% N_2/20% O_2 (right) atmospheres. Four runs are plotted for each.

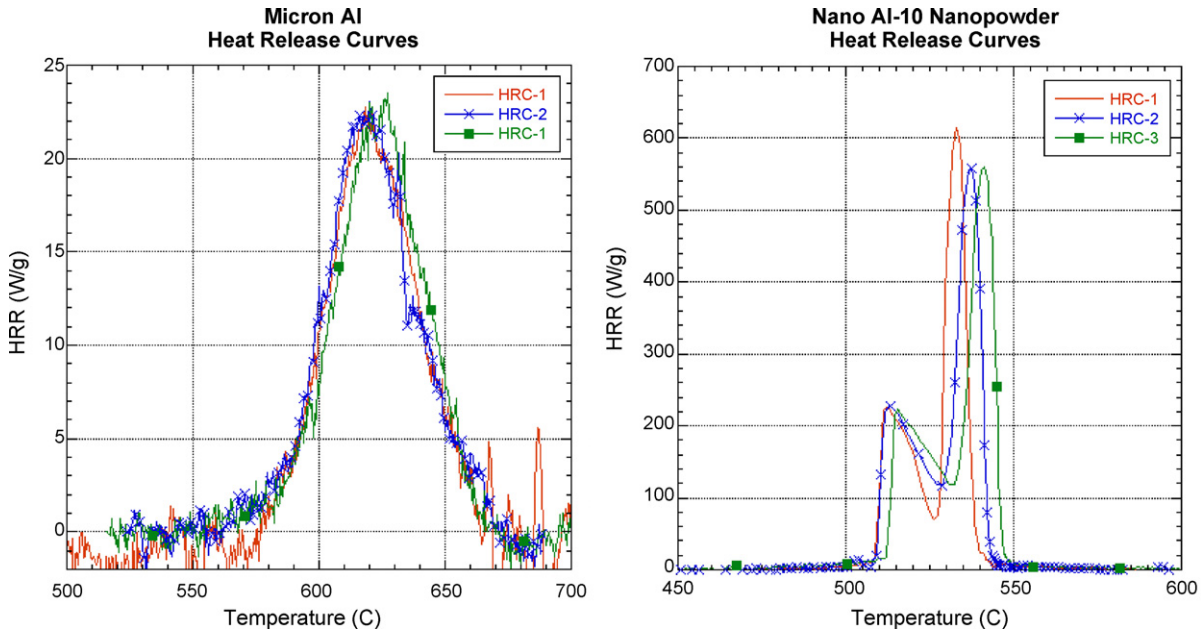

Fig. 7. Heat release rate curves, Micron Al (left), and Nano Al-10 (right). Three runs are plotted for each.

sample, it makes sense that weight gain due to AlN formation would be observable under these conditions while no significant weight gain occurred with the Micron-Al sample. Recall that the PCFC method does not detect heat release caused by the formation of AlN, since no oxygen is consumed. On the other hand, when these samples are heated in air, we observe similar heat release curves (Fig. 8) between the Al-100A and Al-100B samples and peak oxidation/heat release at ~580 °C, with more intense heat release values than that seen with the Micron-Al sample. The lower onset temperature of heat release and higher intensity of reaction are in agreement with results seen elsewhere for nanoscale Al particles [5]. Interestingly, we find a shoulder on the heat release signal on the low temperature side. As we will see, this feature will become even more pronounced at smaller particle sizes.

While these total heat release values (average values of 7.4 and 9.8 kJ/g for A and B, respectively) are larger than the Micron-Al sample, they are still significantly smaller than the either the theoretical value (31 kJ/g Al) or recent experimental value [5] (23 kJ/g Al), which again implies that incomplete oxidation occurred under these experimental conditions. The estimates of the extent of oxidation using heat release again differ somewhat from those calculated from the mass increase, but both agree that the majority of the aluminum metal is not oxidized under these conditions. We would anticipate that the estimates obtained using the mass increase would be larger than those from the heat release (calculated from the oxygen depletion), since formation of AlN contributes only to the former. Actually, this may be advantageous since the difference between the two measurements allows us to separate the contributions to the overall oxidation of aluminum particles in air

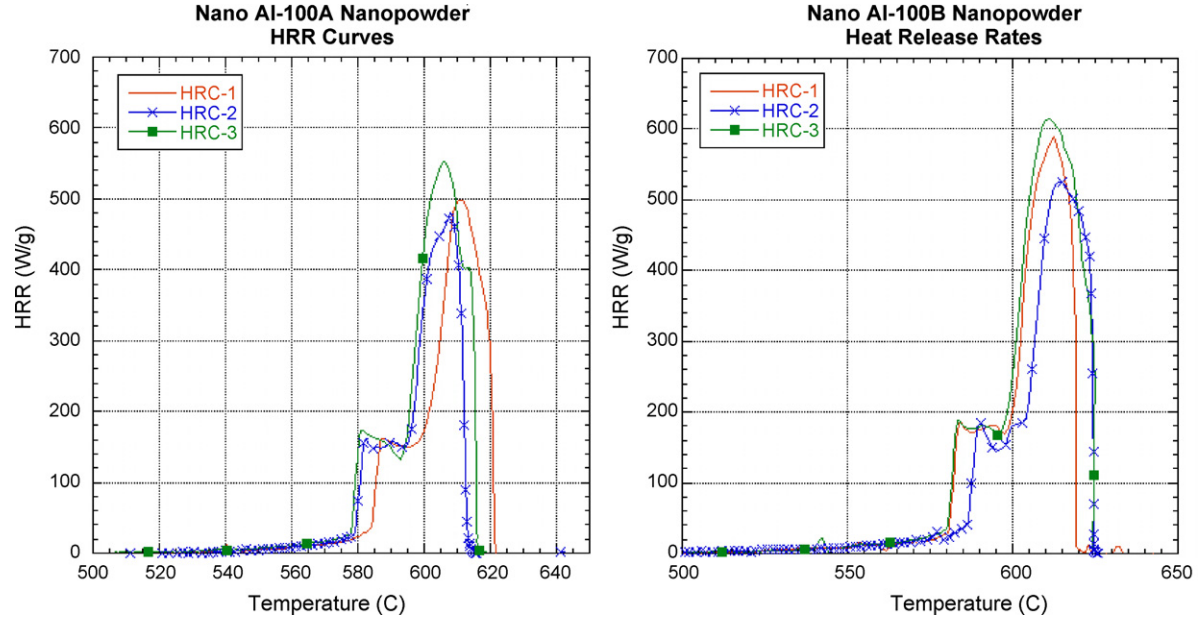

Fig. 8. Heat release rate curves, Nano Al-100A (left) and Nano Al-100B (right). Three runs are plotted for each.

resulting from formation of Al_2O_3 and AlN. Finally, we find that the sample appearance after the test conditions is also consistent with incomplete oxidation of the particles, in that a grey sample with white coloration was noted rather than a completely white sample.

As mentioned above, the fraction of the particle mass contributed by the oxide shell begins to become significant when the particle size is decreased to the nanoscale. Although a pre-existing oxide layer is present on these particles, this fact cannot explain quantitatively that the observed heat release was indicative of incomplete aluminum oxidation. Specifically, if we calculate the amount of Al in a 100 nm particle with an assumed 3 nm Al_2O_3 shell (using literature bulk densities for Al and Al_2O_3) [25] we determine that these starting particles were ~80 wt.% Al, and ~20 wt.% Al_2O_3. Even taking this into account, the fact that the measured extent of reaction is significantly less than 80% still implies that oxidation of the active aluminum content is incomplete.

Turning our attention to the results for the Nano Al-10 powder found in Table 1, we again observe no heat release/oxygen consumption under nitrogen, but do observe weight gain at the end of the experiment, even more so than that observed for the Nano Al-100A and Nano Al-100B powders. This makes sense in that the Nano Al-10 powder, which is on average 10–20 nm in size, has even more surface area than the 100 nm aluminum powders. Again, any heat release that occurs from AlN formation will not be detected by PCFC. When the sample is heated in air (Fig. 7, right) we observe a pronounced two peak curve with peak heat release events at 515 and 535 °C. This behavior seems reminiscent of the results for the 100 nm powders, where we saw a single peak with a prominent shoulder at lower temperatures. The fact that we now see two peaks in the present case implies that the oxidation mechanism that generated the shoulder in the 100 nm case has become even more important here. This observation is consistent with the multi-step oxidation mechanism proposed by Trunov et al. [2], where the first oxidation step involves diffusion-controlled growth of an amorphous oxide layer, followed by a second step characterized by a phase transition to γ-Al_2O_3. Since γ-Al_2O_3 is more dense than the amorphous phase, platelets form and expose some of the aluminum core. The exposed metal then rapidly oxidizes. Although for micron-sized particles the initial diffusion-controlled reaction was observed to be slow compared to the oxidation rate observed immediately following the phase transition [2], these results suggest that the two oxidation steps may become increasingly competitive as the particle size is decreased.

Referring to Table 1, we find that the measured heat release for the Nano Al-10 powder is again lower than the theoretical value, implying incomplete oxidation/combustion. This is supported by the extent of reaction estimated from the measured char yield. Here again we find that the estimate of the extent of reaction obtained from the mass increase is larger than that from the heat release, since formation of AlN can contribute to the former. Interestingly, the amount of mass gain and heat release are lower than those observed for the 100 nm Al powders, which is the opposite trend of increasing mass gain and heat release that we had observed in going from micron-sized to 100 nm aluminum powders. However, this can be explained by considering the contribution of the pre-existing oxide shell. A 10 nm diameter aluminum particle with an assumed 3 nm oxide shell would be only ~20 wt.% aluminum and 80 wt.% oxide (again assuming bulk densities) [25]. So when looking at our estimates of oxidation by mass gain and heat release (Table 1), this number is in good agreement with the observed extent of reaction, which points to nearly complete combustion of the remaining active aluminum for this sample. This is noteworthy considering that the majority of the sample was already oxidized prior to heating due to the passivating oxide shell that spontaneously forms in air.

We now examine our final sample, Nano Al-OA, the 30 nm aluminum nanoparticles protected by an oleic acid coating. When considering the heat release for these samples one must keep in mind that this particle has mixed metal and organic components which may react with each other as well as with oxygen, and therefore the behavior is expected to be more complex than for the above mentioned aluminum samples. It is helpful to first examine the heat release of the organic portion of these particles under nitrogen pyrolysis. Since the aluminum will not be volatile under these temperatures, it will not reach the combustor, hence all of the signal should arise from the oleic acid coating. In Fig. 9(left), we find that under nitrogen two peaks of heat release are observed for the Nano Al-OA sample (Fig. 9, left). This may suggest that the oleic acid bound to the aluminum breaks up into two molecules. We speculate that there could be two types of oleic acid on the aluminum nanoparticle surface (chemisorbed and physisorbed). The physisorbed oleic acid would account for the first peak at 150–350 °C, and then the chemisorbed oleic acid would pyrolyze between 350 and 500 °C. An alternate hypothesis that the first peak would be from a bond breakage at the cis-alkene on oleic acid, and the second peak would be from the rest of the oleic acid fragment still bound to the aluminum surface. Further work will clearly be needed to clarify this issue.

The char yield under these pyrolysis conditions was 61%, indicating that the nanoparticles are at least 39% organic in content, but we must take this as a lower boundary for two reasons. First, the aluminum may pick up weight from reaction with nitrogen (AlN formation) as the organic protecting layer is removed. Secondly, we cannot rule out the possibility that some sort of char has been left behind under these conditions, particularly since the sample is black in appearance at the end of the test, and, aluminum oxide is known to be a coking (charring) catalyst [31–34]. Since we know that the sample is at least 39% organic, we would expect to see approximately 40% of the heat release observed for oleic acid, which should give a value of 12.5 kJ/g. Instead we observe only 8.3 kJ/g, which would correspond to combustion of only 23% of the sample mass, or about half of the organic content. This may indicate that some of the organic coating formed by the sonochemical process to make this sample contains sufficient oxygen content to allow the aluminum sample to self-oxidize under pyrolysis conditions, thereby lowering the oxygen consumption detected in the apparatus. On the other hand, formation of a carbon-rich char layer would trap some of the potential heat release (from oleic acid) in the condensed phase and would thus prevent it from being pyrolyzed and carried to the 900 °C combustion furnace. At this point, these explanations are still speculative. Nevertheless, these data provide a valuable comparison to the results obtained in air.

Under air, we observe different heat release behavior for the Nano Al-OA sample, shown in Fig. 9(right). In the same temperature region observed under nitrogen pyrolysis conditions (150–550 °C, heat release on left axis), we only observe one broad peak of heat release (peak #1 in Table 1) in air rather than the two seen under nitrogen. However, we also observe a much sharper heat release event around 600 °C (peak #2 in Table 1, heat release on right axis from 550 to 700 °C). In Fig. 10, we show an expanded view of peak #2 and find that this signal is actually a doublet, very similar in shape to that observed in the 10 nm sample discussed above. The observed temperature range for this feature for these 30 nm particles is only slightly lower than that for the 100 nm samples above. Since this doublet is similar in shape and onset temperature to that observed for other nano-aluminum samples, it seems clear that this signal is due to Al oxidation. It is interesting that at temperatures higher than peak #1, we see little activity until the onset of Al oxidation near 600 °C. This, combined with the fact that peak #2 is so similar to the signals observed for conventional nanoparticles implies that following removal of the organic passivation layer, the nanoparticles

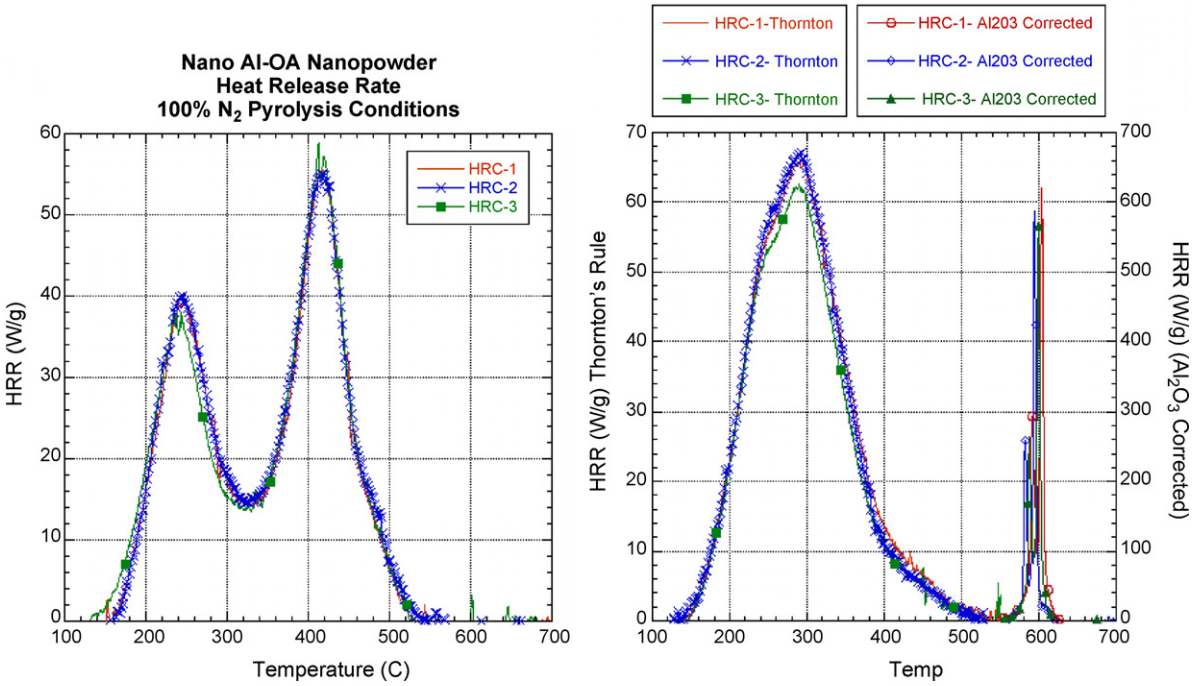

Fig. 9. Heat release rate curves, Nano Al-OA in nitrogen (left) and Nano Al-OA in air (right). At right, two axes are shown; one corresponding to organic combustion according to Thornton's rule and the other corresponding to oxidation of Al to form Al_2O_3 (see text). Three runs are plotted for each.

become oxide-passivated. At higher temperatures, they then follow the same oxidation mechanisms discussed above for conventional particles.

At this point the relative contributions to peak #1 from combustion of the organic shell and from oxidation of exposed aluminum once the organic shell is removed are unclear. In Table 1, we list two heat release values for peak #1 for the Nano Al-OA sample; an organic heat release value that assumes the detected oxygen consumption is entirely due to organic combustion, and an Al oxidation value that assumes peak #1 is solely a result of Al_2O_3 formation. Although at present we cannot precisely determine the relative contribution of each, we can see that the oxygen consumption corresponding to peak #1 is only ~10% larger than that measured for the sample under nitrogen pyrolysis conditions, suggesting that even in air the majority of this peak comes from the organic component of the nanoparticle.

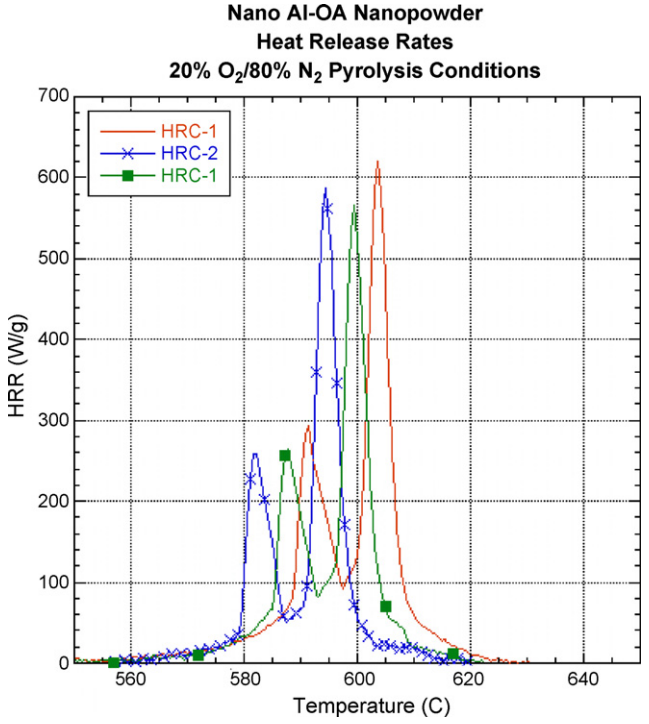

Fig. 10. Expanded view of heat release peak #2 for Nano Al-OA in air. Three runs are plotted.

Returning to peak #2, we note that the heat release associated with peak #2 is only 1.9 kJ/g, and can be explained by oxidizing a quantity of Al metal that represents just 6% of the sample mass. Even if we assume that 10% of peak #1 is due to Al oxidation as mentioned above, the heat release can still be explained by combustion of only ~14% of the sample mass. This seems odd, since this extent of oxidation is somewhat lower than that observed for larger 100 nm particles (refer to Table 1). It is similar to the extent of oxidation observed for 10 nm particles, but there ~80% of the sample aluminum was already consumed by the naturally occurring oxide shell. This observation may be an indication that during combustion of the organic layer, a sort of char is left behind which continues to protect the aluminum to some degree. Alternatively, this may be evidence that the Nano Al-OA particles still possess some oxide. Indeed, this possibility has been suggested elsewhere [10]. Whatever the reason, these results are clearly consistent with incomplete oxidation of the sample, a finding that has been confirmed using XRD on samples after heating to 700 °C [10].

4. Conclusions

The PCFC method was used to measure the heat release of five aluminum samples through the use of oxygen consumption calorimetry, and some general trends were observed.

1. For conventional oxide-passivated aluminum particles, we find (in agreement with other researchers) [5] that the onset temperature for reaction decreases with particle size. For micron-sized particles, reaction is observed between ~600 and 650 °C. By the

time the particle size has decreased to 10 nm, the threshold has been lowered to ~500–550 °C.
2. The extent of reaction for temperatures under 700 °C is observed to increase as the particle size is decreased. Combustion of micron-size particles is far from complete, but the extent of oxidation increases for 100 nm samples, and all of the active aluminum content of smaller 10 nm particles is fully oxidized or nearly so. However, for such small sizes we note the majority of the aluminum is already "consumed" by the naturally occurring oxide layer.
3. As aluminum particles are heated, we detect oxygen consumption occurring in two distinct peaks. Following previous work [2], we assign these to a slower diffusion-controlled oxidation step and more rapid oxidation step following a phase change in the Al_2O_3 layer. In micron-scale particles, only one peak is readily visible, presumably from the faster second step. As the particle size is decreased to the nanoscale, the diffusion-controlled step becomes more prominent, and for 10 nm particles, the two steps become competitive.
4. For the aluminum nanoparticles passivated by oleic acid (30 nm average size), the observed oxidation behavior is more complex than that observed for conventional nanoparticles. At temperatures between 200 and 500 °C the organic coating combusts. Following removal of the organic passivation layer, the nanoparticles appear to become oxide-passivated (or char-passivated) and subsequently behave like conventional aluminum nanoparticles at higher temperatures.

The data collected from the PCFC does give us some insight into the reactions between Al nanoparticles and oxygen. Although we are not able to push the samples to full oxidation in the conditions used in the PCFC (700 °C), we are still able to observe and measure amounts of oxidation in bulk aluminum powders. However, the data suggests that under typical air mixtures the aluminum will react with oxygen and nitrogen at elevated temperatures. The formation of Al_2O_3 and AlN are both exothermic, something that would be observed with DSC or oxygen bomb calorimetry. Of course, since both reactions would occur simultaneously in an air atmosphere, a separation strategy would need to be employed in order to quantify the relative contributions. The PCFC data may indicate that the maximum amount of Al_2O_3 that can be formed up to 700 °C is that measured in this paper – with the difference of mass gain and potential heat release coming from AlN rather than Al_2O_3. The Nano Al-OA nanoparticle presents an interesting system in that it gives off heat from hydrocarbon combustion (the oleic acid coating) at very low temperatures (as early as 150 °C) and then again at elevated temperatures once the aluminum activates. The complexity of this system indicates that more work is needed to understand how organic molecules and metals behave at their interface under combustion conditions, and, how that influences combustion/oxidation behavior.

The challenge of quantifying nanoscale behavior on a bulk sample is not fully solved with the use of PCFC, but information is gained which should be useful in the development of new nanoscale aluminum powders, or new techniques which can combine traditional calorimetry with evolved gas and condensed phase analysis to provide the quantification of nanoparticle performance which is needed to move this field of research forward. In future work we hope to begin chemical analysis of the materials left after pyrolysis events to better characterize the chemical reactions that have occurred and further explore understand how nanoparticle chemistry affects the formation rates of alumina and aluminum nitride. Further, we plan to analyze these samples under Ar gas rather than N_2 so that we can better quantify the AlN formation observed in the current results.

Acknowledgments

The authors would like to thank Mary Galaska for collecting the PCFC data, and the Defense Threats Reduction Agency (DTRA) for funding under grant #HDTRA-07-1-0026. Also, we would like to thank Chris Bunker of AFRL/RZPF (Fuels Branch) for technical discussions and support on use of XRD and TEM instrumentation to characterize the nanoparticles.

References

[1] P.W. Cooper, Explosives Engineering, Wiley–VCH, New York, 1996.
[2] M.A. Trunov, M. Schoenitz, X. Zhu, E.L. Dreizin, Combust. Flame 140 (2005) 310–318.
[3] L.P.H. Jeurgens, W.G. Sloof, F.D. Tichelaar, E.J. Mittemeijer, J. Appl. Phys. 92 (2002) 1649–1656.
[4] L.P.H. Jeurgens, W.G. Sloof, F.D. Tichelaar, E.J. Mittemeijer, Thin Solid Film 418 (2002) 89–101.
[5] J. Sun, M.L. Pantoya, S.L. Simon, Thermochim. Acta 444 (2006) 117–127.
[6] A.P. Il'in, A.A. Gromov, G.V. Yablunovskii, Combust. Explo. Shock Waves 37 (2001) 418–422.
[7] R.J. Jouet, A.D. Warren, D.M. Rosenberg, V.J. Bellitto, K. Park, M.R. Zachariah, Chem. Mater. 17 (2005) 2987–2996.
[8] R.J. Jouet, R.H. Granholm, H.W. Sandusky, A.D. Warren, in: M.D. Furnish, M. Elert, T.P. Russell, C.T. White (Eds.), Shock Compression of Condensed Matter – 2005, Am. Inst. Phys., 2006.
[9] C.E. Bunker, J.K. Karnes, J. Am. Chem. Soc. 126 (2004) 10852–10853.
[10] K.A.S. Fernando, M.J. Smith, B.A. Harruff, W.K. Lewis, E.A. Guliants, C.E. Bunker, J. Phys. Chem. C 113 (2009) 500-503.
[11] A.C. Templeton, W.P. Wuelfing, R.W. Murray, Acc. Chem. Res. 33 (2000) 27–36.
[12] R.W.J. Scott, O.M. Wilson, R.M. Crooks, J. Phys. Chem. B 109 (2005) 692–704.
[13] A.C. Templeton, M.J. Hostetler, C.T. Kraft, R.W. Murray, J. Am. Chem. Soc. 120 (1998) 1906.
[14] Y.-S. Shon, G.B. Dawson, M. Porter, R.W. Murray, Langmuir 18 (2002) 3880.
[15] M.A. Trunov, S.M. Umbrajkar, M. Schoenitz, J.T. Mang, E.L. Dreizin, J. Phys. Chem. B 110 (2006) 13094.
[16] P.M. Hergenrother, C.M. Thompson, J.G. Smith, J.W. Connell, J.A. Hinkley, R.E. Lyon, R. Moulton, Polymer 46 (2005) 5012–5024.
[17] J.L. Jurs, J.M. Tour, Polymer 44 (2003) 3709–3714.
[18] H. Zhang, R.J. Farris, P.R. Westmoreland, Polymer 36 (2003) 3944–3954.
[19] R.N. Walters, R.E. Lyon, J. Appl. Polym. Sci. 87 (2002) 548–563.
[20] R.E. Lyon, R.N. Walters, J. Anal. Appl. Pyrol. 71 (2004) 27–46.
[21] B. Schartel, K.H. Pawlowski, R.E. Lyon, Thermochim. Acta 462 (2007) 1–14.
[22] A.B. Morgan, M. Galaska, Polym. Adv. Technol. 19 (2008) 530–546.
[23] W.M. Thornton, Philos. Mag. 33 (1917) 196–203.
[24] E.H. Battley, in: R.B. Kemp (Ed.), Handbook of Thermal Analysis and Calorimetry, vol. 4, Elsevier, Amsterdam, 1999, pp. 219–265.
[25] CRC Handbook of Chemistry and Physics, CRC Press, ISBN 978-1420066791.
[26] P.R. Watson, M.A. Van Hove, K. Hermann, J. Phys. Chem. Ref. Data 5 (1994) 1–1341.
[27] L. Keffler, J.H. McLean, J. Soc. Chem. Ind. (1935) 178–185.
[28] A.G. Emery, F.G. Benedict, Am. J. Physiol. 28 (1911) 301–307.
[29] N. Glumac, J. Appl. Phys. 98 (2005) 053301.
[30] R.K. Paul, K.-H. Lee, B.-T. Lee, H.-Y. Song, Mater. Chem. Phys. 112 (2008) 562–565.
[31] N. Cinausero, N. Azema, M. Cochez, et al., Polym. Adv. Technol. 19 (2008) 701–709.
[32] M. Soyama, K. Inoue, M. Iji, Polym. Adv. Technol. 18 (2007) 386–391.
[33] A. Laachaci, M. Chochez, E. Leroy, M. Ferriol, J.M. Lopez-Cuesta, Polym. Degrad. Stab. 92 (2007) 61–69.
[34] F. Laoutid, L. Ferry, J.M. Lopez-Cuesta, A. Crespy, Polym. Degrad. Stab. 82 (2003) 357–363.